Kobe University Repository : Kernel

PDF issue: 2026-11-12

Tracking spatiotemporal variations in porewater dissolved organic matter in a planted mangrove chronosequence using FT-ICR MS

Sumioka, Ryu ; Rodtassana, Chadtip ; Poungparn, Sasitorn ; Nishimura, Hiroshi ; Shinozuka, Ken'ichi ; Ohtsuka, Toshiyuki ; Fujitake,…

(Citation)
Organic Geochemistry,217:105208

(Issue Date)
2026-07

(Resource Type)
journal article

(Version)
Version of Record

(Rights)
© 2026 The Authors. Published by Elsevier Ltd.
This is an open access article under the Creative Commons Attribution-NonCommercial 4.0 International license

(URL)
https://hdl.handle.net/20.500.14094/0100503562

Organic Geochemistry 217 (2026) 105208

Contents lists available at ScienceDirect

Organic Geochemistry

journal homepage: www.elsevier.com/locate/orggeochem

Tracking spatiotemporal variations in porewater dissolved organic matter in a planted mangrove chronosequence using FT-ICR MS

Ryu Sumioka [a], Chadtip Rodtassana [b], Sasitorn Poungparn [b], Hiroshi Nishimura [c], Ken'ichi Shinozuka [d], Toshiyuki Ohtsuka [d], Nobuhide Fujitake [a], Morimaru Kida [a,*]

[a] Soil Science Laboratory, Graduate School of Agricultural Science, Kobe University, 1-1 Rokkodai, Nada, Kobe, Hyogo 657-8501, Japan
[b] Faculty of Science, Chulalongkorn University, Bangkok 10330, Thailand
[c] Research Institute for Sustainable Humanosphere (RISH), Kyoto University, Gokasho, Uji, Kyoto 611-0011, Japan
[d] Institute for Advanced Study, Gifu University, 1-1 Yanagito, Gifu City, Gifu 501-1193, Japan

ARTICLE INFO

Associate Editor: Yina Liu

Keywords:
Dissolved organic matter
FT-ICR MS
Chronosequence
Spatiotemporal variability
Mangrove
Dissolved organic sulfur
Molecular diversity

ABSTRACT

Mangroves are important sources of dissolved organic matter (DOM) that contribute to marine carbon sequestration. Porewater acts as a key intermediate reservoir through which mangrove-derived DOM is mobilized and transported to adjacent coastal waters. Despite this importance, the spatiotemporal variability in porewater dissolved organic carbon (DOC) concentration and molecular composition within mangrove ecosystems remains poorly understood. This study applied a chronosequence approach across four mangrove plantations of different ages (10–18 years) in Thailand to investigate the spatiotemporal variability in DOC concentration and molecular composition using ultrahigh-resolution mass spectrometry (FT-ICR MS). Temporal variation was inferred from the10–18-year age sequence, including mudflats as a reference, while spatial variation was assessed along seaward-to-landward transects within each plantation. DOC concentrations increased landward but showed no significant dependence on forest age, indicating that porewater DOC is primarily regulated by spatial gradients associated with tidal dilution and vegetation distribution rather than by forest development. In contrast, DOM molecular composition responded to both distance from the seaward edge and forest age. At landward sites in older forests, the relative abundances of aromatic and sulfur-containing compounds increased, coinciding with a molecular index indicative of sulfidic porewater. The enrichment of sulfur-containing compounds and high values of the molecular index are consistent with abiotic sulfurization of porewater DOM under sulfate-reducing redox conditions. This study shows that mangrove forest development alters the quality of porewater DOM, with implications for the contribution of mangrove-derived recalcitrant carbon to porewater pools, carbon cycling, and long-term carbon persistence in blue carbon ecosystems.

1. Introduction

Mangroves play important roles as both sinks and sources of carbon in subtropical to tropical coastal areas (Dittmar et al., 2006; Bouillon et al., 2008; Alongi, 2020; Reithmaier et al., 2023). Although mangroves occupy only 0.5% of the world's coastal areas (based on our calculations using recent global mangrove and coastline datasets (Bauer et al., 2013; Jia et al., 2023)), they contribute approximately 13% of the organic carbon (OC) and 28% of the dissolved inorganic carbon (DIC) exported from coastal zones to the ocean (Alongi, 2020). This carbon flux is primarily facilitated by tidal pumping, which drives the exchange of porewater enriched with dissolved organic matter (DOM), DIC, and nutrients to coastal waters (Maher et al., 2013; Stieglitz et al., 2013; Tait et al., 2016; Mori et al., 2019; Xiao et al., 2023). Mangrove-derived DOM contributes to marine carbon sequestration due to the export of its recalcitrant fraction to the ocean, such as aromatic compounds and dissolved organic sulfur (DOS) (Dittmar et al., 2006; Mori et al., 2019; Santos et al., 2021; Knoke et al., 2024). The persistence of these compounds is attributed not only to the inherent structural stability of aromatic rings against microbial cleavage (Dittmar, 2015) and the resistance of sulfurized molecules to enzymatic hydrolysis (Pohlabeln et al., 2017), but also to the high molecular complexity and diversity of the exported DOM pool. Specifically, it is hypothesized that the extremely low concentrations of individual molecular species and their

* Corresponding author.
E-mail address: morimaru.kida@people.kobe-u.ac.jp (M. Kida).

https://doi.org/10.1016/j.orggeochem.2026.105208
Received 12 January 2026; Received in revised form 9 March 2026; Accepted 1 April 2026
Available online 3 April 2026
0146-6380/© 2026 The Authors. Published by Elsevier Ltd. This is an open access article under the CC BY-NC license (http://creativecommons.org/licenses/by-nc/4.0/).

diverse structures reduce the encounter rate between specific substrates and microbes, thereby limiting their degradation (Arrieta et al., 2015; Dittmar, 2015).

Beyond its role in carbon sequestration, mangrove-derived DOM also influences coastal ecosystem functioning through its distinctive molecular composition. It exhibits higher aromaticity and stronger light absorption than coastal DOM (Dittmar et al., 2006; Tremblay et al., 2007; Kida et al., 2019b), thereby attenuating solar radiation and influencing primary production (Jaffé et al., 2008). Moreover, it affects biogeochemical processes such as pH buffering and metal speciation, as well as the microbial food web (Jaffé et al., 2008). These ecological functions are fundamentally controlled by the complex molecular composition of DOM (Tanentzap and Fonvielle, 2024). Greater molecular diversity in DOM expands the range of available resource niches, supporting more diverse and functionally redundant microbial communities, and thereby stabilizing DOM-mediated ecosystem processes, such as organic carbon decomposition (Tanentzap et al., 2019; Wen et al., 2024; Freeman et al., 2025). Therefore, investigating the concentration, molecular composition, and diversity in DOM is essential for understanding its biogeochemical behavior in coastal ecosystems.

The composition of porewater DOM in mangroves may change with forest age (Ray et al., 2023; Mouras et al., 2025) and estuarine mixing (Mori et al., 2019; Xiao et al., 2023), which may together drive its spatiotemporal variability (Kida et al., 2019b). For instance, increasing forest age has been associated with higher humification degrees (Mouras et al., 2025) and elevated DOM concentrations in porewater (Ray et al., 2023). Similarly, humification degrees and DOM concentrations were higher landward within a Chinese mangrove forest, due to stronger dilution at seaward sites (Xiao et al., 2023). Such spatiotemporal heterogeneity, often linked to terrestrial and anthropogenic inputs, is well-documented for sedimentary organic matter in estuarine systems (He et al., 2018; Zhang et al., 2021). However, the spatiotemporal variability in porewater DOM concentration and composition within mangrove ecosystems remains poorly understood, despite DOM being the most active component of carbon cycling. Recent studies have advanced our understanding of the molecular composition of water-extractable organic matter in mangrove sediments (Wang et al., 2024; Chen et al., 2025), and this method can be extended to study (pseudo) DOM. However, extractions can influence the composition of recovered organic matter fractions, as for instance organic matter solubility differs markedly between freshwater and saline conditions (Kida et al., 2017). From this perspective, only direct field sampling of porewater DOM enables its characterization under in situ conditions. However, porewater sampling in the field involves more complex logistical procedures (i.e., sample preservation and shipping) and thus remains relatively limited in mangrove settings.

To investigate temporal variations in DOM with forest stand age, a chronosequence approach is effective. This method examines sequential changes over time within spatially consistent environments, treating site age as the primary variable (Johnson and Miyanishi, 2008; Walker et al., 2010). In mangrove ecosystems, sedimentary OC content and stock (Walcker et al., 2018; Sharma et al., 2020; Carnell et al., 2022; Ray et al., 2023) and porewater DOM concentrations (Ray et al., 2023) tend to increase with forest age. However, no study has yet applied a chronosequence approach to examine changes in the molecular composition of porewater DOM in mangrove forests.

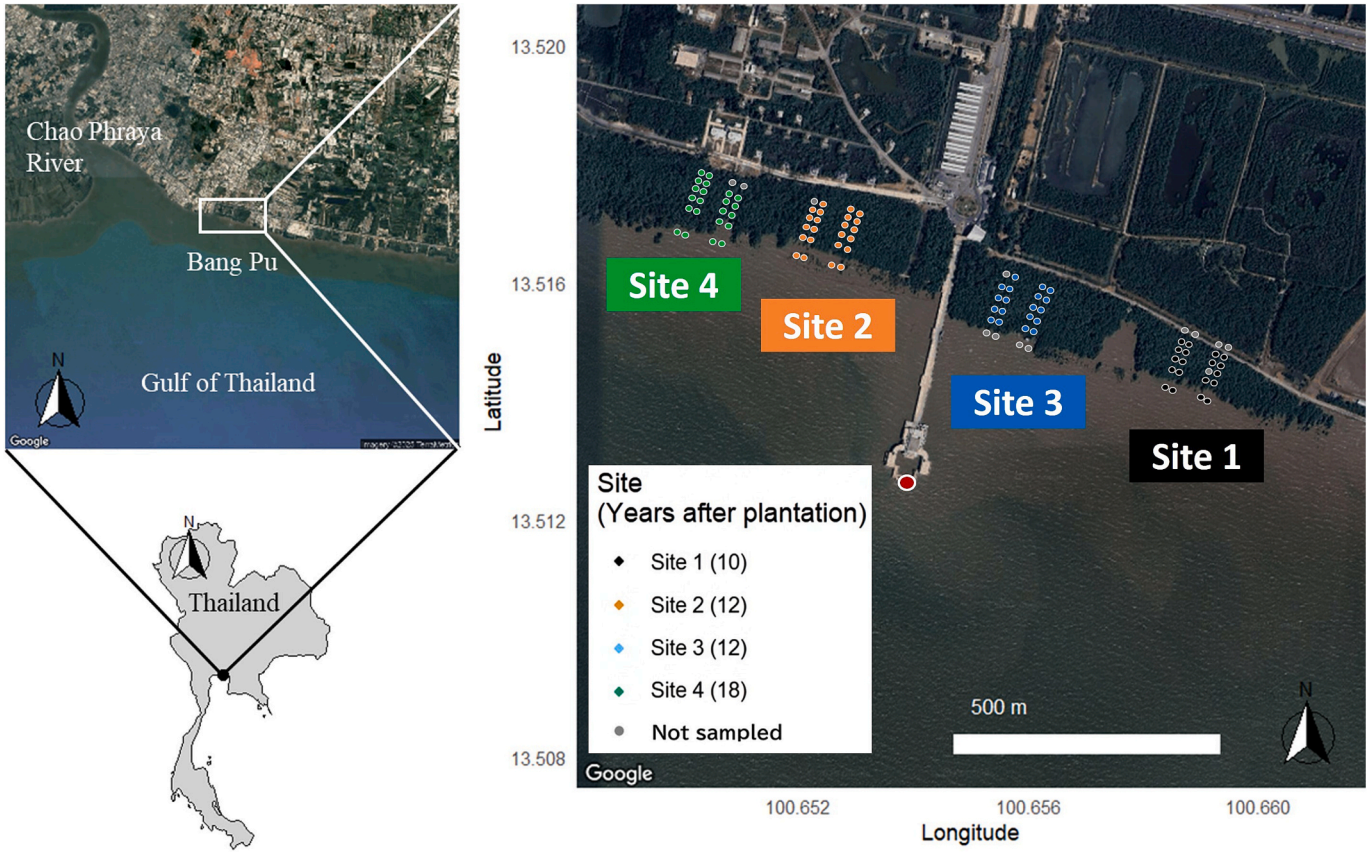


Fig. 1. Sampling sites in the Bang Pu mangrove forest, located at the mouth of the Chao Phraya River in Thailand. The circles represent sampling points, and different colors indicate sites. The outermost circles at each site represent sampling points collected from the mudflat. The gray circles indicate points where sampling could not be conducted due to equipment failure or insufficient distance within the mangrove forest. The red circle denotes the locations where seawater salinity was measured at high tide. The bridge is located in the middle of the area, but the lower part is open, allowing seawater to pass through. Therefore, it does not substantially affect water movement or sediment deposition. (For interpretation of the references to colour in this figure legend, the reader is referred to the web version of this article.)

Our objectives were to investigate the spatiotemporal variations in both the concentration and composition of porewater DOM within mangrove ecosystems. We hypothesized that increases in recalcitrant DOM (aromatic compounds and DOS) would lead to elevated DOC concentrations with increasing forest age and distance from the seaward edge of the mangrove forest. To test this, we collected porewater samples along mudflat-to-inland transects at four sites of different plantation ages (Fig. 1) and analyzed the porewater DOM composition using ultrahigh-resolution Fourier transform ion cyclotron resonance mass spectrometry (FT-ICR MS).

2. Materials and methods

2.1. Study area and sampling

We conducted the study in a mangrove plantation of the Bang Pu Recreation Center, located in the eastern part of Samut Prakan Province, central Thailand (13°31′ N, 100°39′ E) (Fig. 1). The plantation, spanning approximately 14.3 ha as of 2023, is situated near the mouth of the Chao Phraya River, with an average elevation of 4 m above sea level. The vegetation in this area is largely dominated by *Avicennia alba* (Hongwiset et al., 2022). The region has a tropical monsoon climate, with an annual precipitation of 1008 mm, 82.5% of which occurs during the rainy season. The tidal pattern is mixed semidiurnal, with a tidal range from 0 m to 3.4 m (From September 2020 to November 2021, Hydrographic Department, Royal Thai Navy) (Hongwiset et al., 2022). The salinity of seawater sampled near the site at high tide was 23, indicating that the study area was in the brackish zone (Fig. 1).

We conducted field sampling at four sites in early March 2023 during the dry season at low tide. These sites were named according to planting age: Site 1 (10 years), Site 2 (12 years), Site 3 (14 years), and Site 4 (18 years) (Fig. 1). At Site 4, some remnant mangrove trees were present prior to plantation establishment. To minimize variability from environmental heterogeneity, we selected sites located in close proximity near the estuary of the Chao Phraya River, where sedimentary processes and tidal influences are assumed to be relatively uniform at the macroscale. By prioritizing this spatial consistency, we aimed to focus on the effects of forest age on porewater DOM as much as possible. To account for potential variation in mangrove density and DOM composition along the land–sea gradient, we established sampling transects perpendicular to the shoreline, extending approximately 100 m from the seaward edge of the mangrove forest landward. Duplicate transects were established at each site to account for local variability.

We collected porewater at − 5 m (mudflat), 10 m, 30 m, 50 m, 70 m, and 90 m from the seaward edge (0 m) along duplicate transects at each site at a distance of approximately 10–20 m (Fig. 1). We collected porewater using Rhizon samplers (Rhizon CSS, Rhizosphere Research Products) with a 5 cm porous section, which were inserted vertically into the sediment to span the depth from 5 cm to 10 cm below the surface. These samplers are equipped with an inline filter (0.15 μm, polyvinylpyrrolidine and polyethersulfone), enabling simultaneous filtration during sample collection. Each set of porewater extraction required approximately one hour. To further account for spatial heterogeneity, we conducted duplicate sampling (1 m apart) at each sampling point within each transect. In summary, spatial heterogeneity was considered in the sampling design by the four different levels: (1) choosing sites located in close proximity within an estuary dominated by a single mangrove species, (2) establishing duplicate transects at each site, (3) collecting samples along the land–sea gradient, and (4) collecting samples in duplicate at each sampling point. We measured environmental factors (salinity, water temperature, pH, and oxidation–reduction potential [ORP]) using portable meters (salinity: LAQUAtwin Salt, HORIBA, Japan; others: HI991003, HANNA, Romania) at a depth of 7.5 cm from the surface. ORP was temperature-compensated and converted to Eh based on the manufacturer's instructions.

The collected samplers were stored in a cooler and the filtered samples inside the syringes were acidified with 6 M sulfuric acid (H_2SO_4, reagent grade, Fujifilm Wako Pure Chemical Corporation, Japan) to pH 2 within 1–2 days of collection. Sulfuric acid was used for acidification following protocols for nutrient analysis (Burke et al., 2002). We verified that sulfuric acid did not influence the DOM composition by comparing FT-ICR MS spectra of a reference material, Suwanee River Natural Organic Matter (2R101N, purchased from International Humic Substances Society), in duplicate after two-month storage in either pH $2H_2SO_4$ or hydrochloric acid (HCl) (data not shown). Aliquots of porewater samples for DIC measurement were stored in air-tight glass vials without headspace to limit gas exchange. Although chemical preservatives were not added, the samples for DIC analysis were kept in the dark at 4 °C during storage and transport to Japan to minimize microbial activity. All analyses were completed within one month of sample collection.

2.2. Chemical analysis

All glassware underwent acid cleaning by immersion in 0.01 M HCl overnight, followed by heat treatment (at 450 °C for at least four hours), while all plastic containers underwent acid cleaning. We measured DOC, DIC, and total dissolved nitrogen (TDN) concentrations using a total organic carbon analyzer combined with a total nitrogen measuring unit (TOC-L_{CPH}, Shimadzu, Japan), as in Kida et al. (2019). The precision (coefficient of variation) of replicate measurements of standards in replicate vials was 0.45% for DOC and 7.20% for DIC. We measured dissolved inorganic nutrients (NH_4^+, NO_3^-, NO_2^-, PO_4^{3-}, SiO_3^{2-}) using an autoanalyzer (QuAAtro, BLTEC, Japan) employing continuous segmented flow analysis, as in Cao et al. (2019). We re-filtered the samples using a syringe filter (0.22 μm, PES, Millex, Millipore, Germany) before analysis. Dissolved inorganic nitrogen (DIN) was estimated as the sum of NH_4^+, NO_3^-, and NO_2^-, and dissolved organic nitrogen (DON) was estimated as the difference between the TDN and DIN. The reduction efficiency for standard solutions containing nitrate and nitrite was 97%. The coefficient of variation of replicate analysis was 0.42% for NH_4^+, 2.90% for PO_4^{3-}, and 1.03% for SiO_3^{2-}, respectively.

2.3. SPE-DOM extraction and FT-ICR MS

We extracted and desalted DOM for FT-ICR MS using cartridges filled with a styrene–divinylbenzene copolymer (Agilent Bond Elut PPL, 100 mg, United States), following the method established by Dittmar et al. (2008). We mixed duplicate samples at each sampling point in equal carbon amounts, each contributing 0.12 mg C, resulting in a total carbon content of 0.24 mg C for each extraction. This mixing could partially account for spatial heterogeneity of the samples. After mixing samples, we added pH2 ultrapure water (0.01 M HCl) to the mixture to adjust the volume to 50 mL to standardize the concentration and volume across all samples to minimize extraction bias (Kida et al., 2021, 2023). We prepared operational blank extracts by processing 50 mL of pH 2 ultrapure water at the same time as the DOM extraction. The average extraction efficiency was 51.1 ± 7.9% based on a DOC basis (Fig. S1a). We refer to the extracted DOM as solid-phase extracted DOM (SPE-DOM), which was within the analytical window of this study.

We analyzed the samples using a 7 Tesla solariX FT-ICR MS (Bruker Daltonik GmbH, Bremen, Germany) equipped with an electrospray ionization source (ESI, Bruker Apollo II) applied in the negative ionization mode. Before FT-ICR MS, we mixed the SPE-DOM samples with ultrapure water (50:50 v/v) and diluted to a final DOC concentration of 20 mg C L^{-1}, then filtered through a pre-washed syringe filter (0.2 μm, PTFE, Merck, Darmstadt, Germany). A total of 100 single scans with 4 M Word was recorded over a mass-to-charge ratio (m/z) range of 150 to 1800 at the sample injection rate of 180 μL h^{-1}. We optimized ion accumulation time for each sample (0.1–0.45 s) depending on sample spectra intensity.

We performed data processing, molecular formula assignments, and compound category classifications using the software package ICBM-OCEAN (Merder et al., 2020). We internally calibrated the mass spectra using a list of 74 known CHO-only molecular formulas (MFs) spanning the mass range of the samples, with a mass error of less than 0.1 ppm, using Bruker Daltonics Data Analysis software. The method detection limit (MDL) was calculated based on machine noise (Riedel and Dittmar, 2014), and peaks with signal intensities exceeding three times the MDL were retained for analysis. The attribution of MFs followed the method outlined in Kida et al. (2021, 2023), with a maximum elemental composition of $C_{50}H_{100}O_{50}N_4S_3P_1$ and a mass error tolerance of 0.5 ppm. The assigned MFs were isotope-verified and chosen based on a chemical homologous series of CH_2 and O. MFs containing more than three heteroatoms were allowed (e.g., CHONSP, $CHON_2S$, etc.), given possible abiotic sulfurization which randomly incorporates sulfur (S) into organic compounds under anoxic conditions with the presence of reduced S (Gomez-Saez et al., 2016). Peaks detected in at least 3 out of 6 operational blank controls were considered as contaminants and excluded from the sample peaks. Furthermore, we performed manual exclusion of peaks suspected to be contaminants, and we also removed peaks detected in fewer than 5% of the samples. Applying these criteria resulted in the assignment of MFs to 4882 peaks across 43 samples. Then, we removed MFs containing minor isotopes (^{13}C, ^{18}O, ^{15}N, ^{34}S) and those with a difference between the number of oxygen atoms and the number of double bond equivalent (DBE) exceeding 10 (Herzsprung et al., 2014). We used the remaining 3713 MFs for data analysis. Each sample was assigned 2441 ± 118 MFs on average. We calculated the modified aromaticity index (AI_{mod}) and the DBE to evaluate the unsaturation of the MFs (Koch & Dittmar 2016). Then, we calculated the average molecular properties (AI_{mod}, DBE, H/C, O/C, and m/z) as weighted averages based on the peak intensities for each sample. We categorized compound classes according to Merder et al. (2020) as follows: aromatic ($AI_{mod} > 0.5$), highly unsaturated O rich (HU_Or; $AI_{mod} \leq 0.5$ & $H/C < 1.5$ & $O/C \geq 0.5$), highly unsaturated O poor (HU_Op; $AI_{mod} \leq 0.5$ & $H/C < 1.5$ & $O/C < 0.5$), unsaturated ($1.5 \leq H/C$ & DBE $\neq 0$), and saturated (DBE = 0). Similarly, we categorized compound classes based on the containing elements as follows: CHO, CHON, CHOS, CHONS; P was not considered due to its low content. We calculated the relative abundance (%RA) of each compound class as the percentage of the summed abundance of all assigned formulae (Tables S1 and S2).

2.4. Statistical analysis

We conducted all statistical analyses in R version 4.3.1 (https://www.r-project.org/), using the "vegan" package (Oksanen et al., 2022) unless otherwise noted. For each environmental factor, porewater chemistry, and compound class, we conducted statistical comparisons using site and distance from the seaward edge as categorical factors (Tables S3 and S4), due to the limited number of sites (n = 4) and nonlinear spatial patterns of most analyzed parameters along the transects. Due to the limited sample size and high heterogeneity across samples, we used Kruskal–Wallis tests for all comparisons. pH, Eh, and water temperature were excluded from the statistical analysis due to missing values caused by instrument malfunction at Site 1 and Site 3.

Using MFs identified by FT-ICR MS, we calculated the molecular index of sulfidic porewater (I_{SuP}), a proxy recently proposed to assess the contribution of DOM derived from mangrove porewater (Knoke et al., 2024). I_{SuP} is calculated using the relative intensities of 40 sulfur-containing MFs characteristic of mangrove porewater and 40 MFs representing marine-derived DOM (see Knoke et al., 2024 for a detailed list of MFs). I_{SuP} ranges from 0 to 1, and higher values indicate a greater contribution of mangrove porewater-derived DOS in the samples. We also quantified the molecular diversity in SPE-DOM as the effective number of species (ENS) applying concepts from community ecology (Tanentzap et al., 2019), which provides an intuitive and linear metric for comparing molecular diversity across samples. ENS represents the number of equally abundant species (in this case, each MF) required to produce the same diversity as the observed community within a single sample (Jost, 2006). ENS was calculated from the Gini-Simpson index (selected because of its robustness against low-intensity noise (Mentges et al., 2017)), following the equation of Jost (2007): ENS = 1 / (1 − Gini Simpson index). We note two important considerations when applying ENS to relative abundance of MFs. First, because ESI efficiencies can differ among compounds, peak intensities in FT-ICR MS are not directly proportional to true concentrations. Accordingly, ENS should be interpreted as a measure of the chemodiversity in SPE-DOM within a defined analytical window, rather than as a direct analogue of community diversity based on organismal counts. Second, mass spectrometry data are inherently *compositional,* and ENS is not subcompositionally coherent (see our recent review; (Kida et al., 2026)) because it is computed from the relative abundance of MFs and thus a function of the set of MFs included in the analysis. Subcompositional coherence means that relationships among components remain invariant when the composition is restricted to a subset and renormalized; however, ENS generally changes when molecular features are added or removed. Consequently, ENS derived from relative MF abundance may be sensitive to the selection of MFs included in the analysis. Such selection depends on multiple analytical and post-processing steps, including the treatment of peaks near the noise threshold, the efficiency of MF assignment, and subsequent peak filtering (e.g., exclusion of isotopologues or MFs with DBE–O > 10). Nevertheless, ENS values remain comparable among samples provided that all data are processed under identical analytical and filtering criteria.

Finally, we visualized the spatiotemporal changes in the molecular composition of SPE-DOM by non-metric multidimensional scaling (NMDS) based on Jensen–Shannon divergence (Kida et al., 2023). We also conducted a compositional-aware principal component analysis (PCA) after robust centered log-ratio transformation (without low-rank approximation) (Kida et al., 2026), which yielded a broadly similar sample distribution to the NMDS results. However, in the PCA, the first two principal components explained only a small proportion of the variance (23%), limiting the interpretability of the two-dimensional projection. Therefore, we report NMDS results which yielded a sufficiently low stress value (0.119) in the 2D ordination space. Average molecular properties and environmental factors were fitted *post-hoc* onto the 2D ordination space using the envfit function (permutations = 9999, $p \leq 0.01$) provided in the vegan package of R (Oksanen et al., 2022). Because we mixed duplicate samples for solid-phase extraction due to sample limitation, we calculated environmental factors of each sample as weighted averages based on the volume ratios of the mixed duplicate samples.

3. Results

For all figures except the NMDS, we used the mean values and standard deviations of the two transects at each site to facilitate visualization, while acknowledging the inherent variability between paired transects. Reported values in the manuscript are also mean values.

3.1. Porewater chemistry

Porewater salinity ranged from 18 to 25 and differed significantly with distance from the seaward edge ($p < 0.001$, see Tables S3 and S4 for precise sample numbers), exhibiting a clear landward increase (Fig. 2a). Water temperature (27.5 °C to 32.7 °C) and pH (7.0 to 7.5) tended to be higher seaward (Fig. 2b, c). Eh ranged from –36.5 mV to + 77.0 mV, with larger fluctuations along distances from the seaward edge in the oldest site compared to a younger site (Fig. 2d).

DOC concentrations ranged from 7.17 mg C L^{-1} to 24.9 mg C L^{-1} and differed significantly with distance from the seaward edge ($p < 0.01$, Table S4), exhibiting a landward increase with the highest values observed in Site 4 (Fig. 2e). DON concentrations ranged from 0.64 mg N

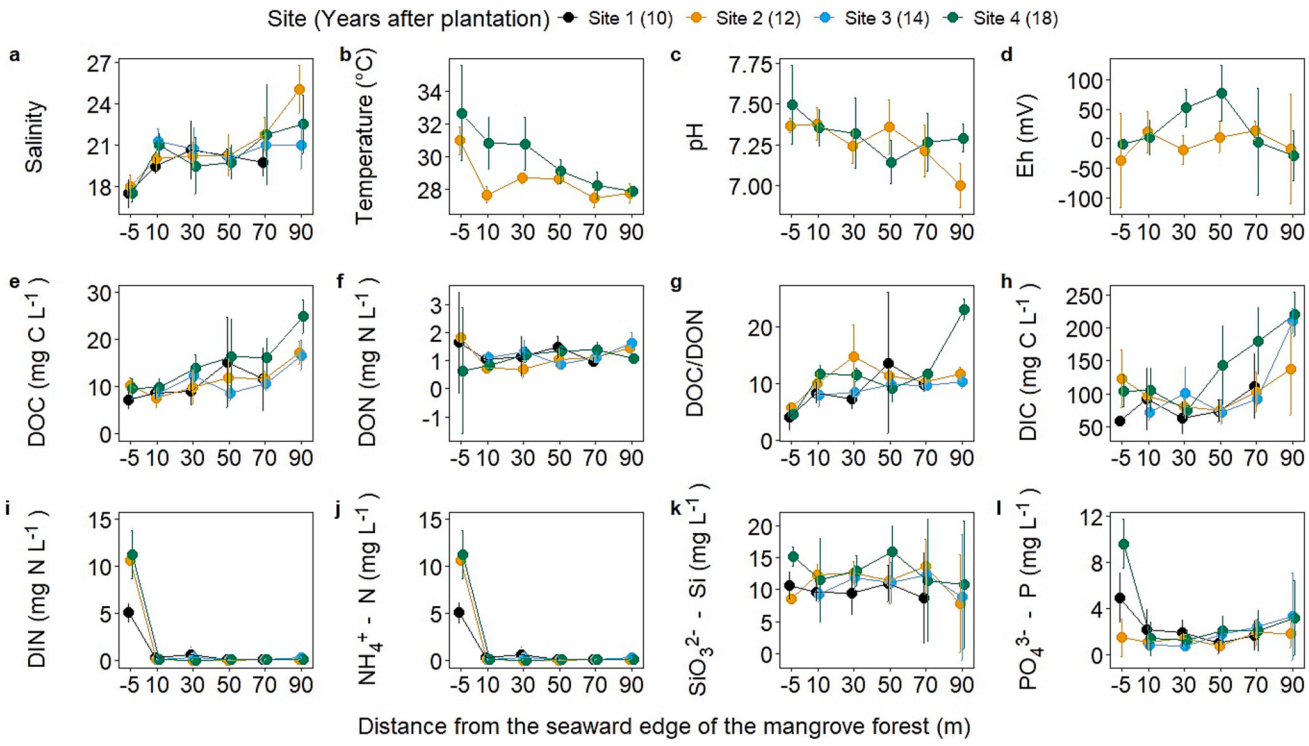


Fig. 2. Environmental factors (a–d) and dissolved carbon and nutrient concentrations (e–l) at various points along the landward distances from the seaward edge of the mangrove forest. Values are presented as means ± standard deviations calculated from the two transects. Due to a malfunction in the portable meter, data for water temperature, pH, and Eh at Site 1 and Site 3 are missing. DOC, dissolved organic carbon; DON, dissolved organic nitrogen; DOC/DON, molar ratio of DOC to DON; DIC, dissolved inorganic carbon; DIN, dissolved inorganic nitrogen.

L^{-1} to 1.82 mg N L^{-1}, showing no clear variation within the mangrove forest (Fig. 2f). DOC/DON ratios ranged generally between 5 and 15, with differences between the mudflat and forest interiors (Fig. 2g), and showed additional variability across forest age ($p = 0.021$, Table S3). DIC concentrations far exceeded DOC concentrations, ranging from 58.4 mg C L^{-1} to 220 mg C L^{-1} (Fig. 2h). Site 4 exhibited a pronounced landward increase and generally higher levels in DIC than the other sites, although the differences were not statistically significant among sites ($p = 0.050$, Table S3). DIN concentrations ranged from 0.065 mg N L^{-1} to 11.3 mg N L^{-1} (Fig. 2i), and ammonium-N accounted for 99% of DIN (Fig. 2j). They varied significantly with distance from the seaward edge ($p < 0.01$, Table S4), showing the highest values in the mudflat and

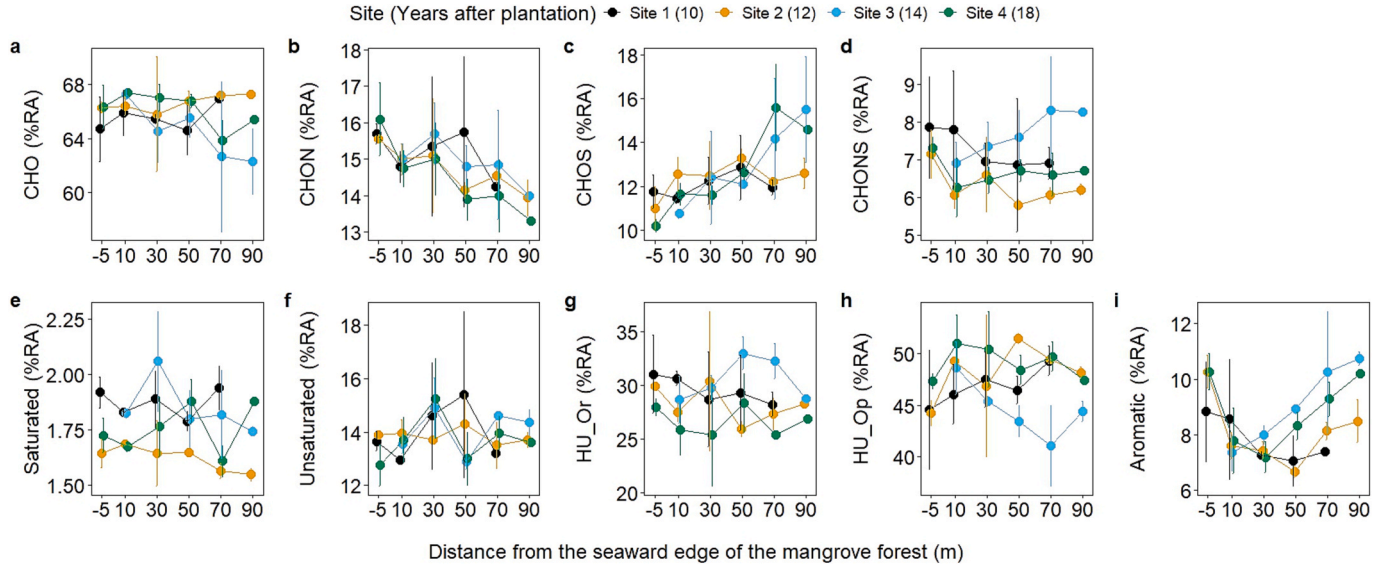


Fig. 3. Relative abundance of each compound group at various points along the landward distances from the seaward edge of the mangrove forest. Values are presented as means ± standard deviations calculated from the two transects. In the upper panels, compounds are classified based on elemental composition and expressed in percent relative abundance (%RA): (a) CHO, containing only carbon, hydrogen, and oxygen, (b) CHON, containing nitrogen, (c) CHOS, containing sulfur, (d) CHONS, containing both nitrogen and sulfur. In the lower panels, compounds are categorized based on their H/C and O/C ratios, double bond equivalent, and modified aromaticity index: (e) saturated, (f) unsaturated, (g) HU_Or, highly unsaturated with O/C ≥ 0.5, (h) HU_Op, highly unsaturated with O/C < 0.5, and (i) aromatic. Please see the main text for further details concerning classification.

lower, relatively constant values within the mangrove forest (average 0.16 ± 0.20 mg N L^{-1}). The concentration of dissolved silica and phosphate ions ranged from 7.74 to 16.0 mg Si L^{-1} and 0.768–9.62 mg P L^{-1} (Fig. 2k, l). There were no significant differences in porewater nutrients across the sites (DIN: $p = 0.90$, NH_4^+: $p = 0.86$, SiO_3^{2-}: $p = 0.20$, PO_4^{3-}: $p = 0.18$, Table S3).

3.2. Molecular composition of SPE-DOM

SPE-DOM composition varied with forest age or distance from the seaward edge (Figs. 3 and 4, Fig. S1). The ranges of intensity-weighted average H/C, O/C, *m/z*, AI_{mod}, DBE, and NOSC were 1.25–1.32, 0.44–0.50, 358–370, 0.23–0.27, 7.05–7.55, and −0.33–-0.11, respectively (Tables S1 and S2).

Among elemental compound classes, CHO accounted for the largest portion, ranging from 62.3 to 67.4% of the total relative abundance (Fig. 3a). CHON and CHOS exhibited similar relative abundances (10–16%) but showed contrasting spatial patterns across sites (Fig. 3b and c). Both compound classes differed significantly with distance from the seaward edge ($p < 0.01$, Table S4), whereas no significant differences were observed among forest ages overall (CHON: $p = 0.77$, CHOS: $p = 0.81$, Table S3). CHON generally decreased landward (Fig. 3b), while CHOS generally increased landward specifically at the older sites (Site 3 and 4). The younger sites (Site 1 and 2) displayed lower spatial variation in the elemental composition compared to older sites (Fig. 3b and c). CHONS accounted for the smallest portion, ranging from 5.8 to 8.3% (Fig. 3d). Among compound groups classified by H/C and O/C ratios, highly unsaturated compounds (HU_Or and HU_Op) were most abundant, together accounting for 73–78%, with larger contributions from HU_Op (Fig. 3g and h). Aromatic compounds ranged from 6.7 to 10.8% and differed significantly with distance from the seaward edge ($p < 0.01$, Table S4). Specifically, they increased landward at the older sites (Site 3 and 4), with the exception of the mudflat (Fig. 3i).

In Bang Pu, I_{SuP} ranged from 0.12 to 0.31 and differed significantly among forest ages ($p < 0.01$, Table S3) and distances from the seaward edge ($p < 0.01$, Table S4), exhibiting pronounced landward increases at the older sites (Site 3 and 4) (Fig. 4a). I_{SuP} values are comparable to the range of 0.15 to 0.20 reported for other mangrove fringes (Knoke et al., 2024), except for the notably higher values at the landward sites. The diversity in SPE-DOM quantified as ENS ranged from 645 to 1096, showing significant differences with forest age ($p < 0.01$, Table S3) and distance from the seaward edge ($p = 0.047$, Table S4), with increases observed landward in Site 3 and 4 (Fig. 4b).

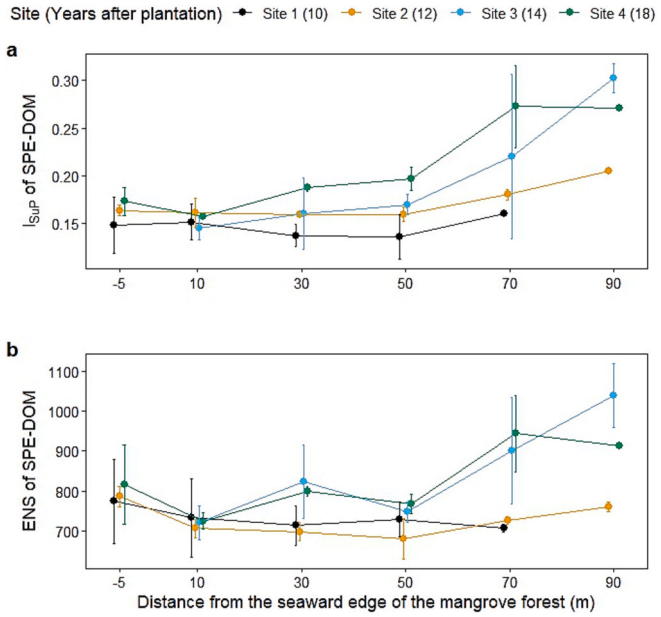


Fig. 4. (a) The molecular index of sulfidic porewater (I_{SuP}) (Knoke et al., 2024) of solid phase-extracted dissolved organic matter (SPE-DOM) at various points along the distance from the seaward edge of the mangrove forest. (b) The effective number of species (ENS) of solid phase-extracted dissolved organic matter (SPE-DOM) at various points along the landward distances from the seaward edge of the mangrove forest. Values are presented as means ± standard deviations calculated from the two transects.

NMDS based on the FT-ICR MS relative peak intensities showed general shifts in the SPE-DOM composition with the distance along the transect, albeit with relatively high variability (Fig. 5). Especially, the landward points (70 and 90 m) at the older sites (Site 3 and 4) were distinct from all other sampling locations. These points were characterized by higher ENS and I_{SuP} values (Fig. 4a and b), along with an increased relative abundance of aromatic compounds (Fig. 3c and i). They also exhibited elevated DIC concentrations, AI_{mod} and DBE values (Fig. 5).

4. Discussion

In surface porewaters of the Bang Pu mangrove, the seaward-to-landward environmental gradient exerted a strong control on porewater DOC concentrations. DOC increased landward (Fig. 2e, Table S4), whereas no significant differences were observed among forest ages (Table S3), partly rejecting our working hypothesis. The landward increase in DOC likely reflects enhanced carbon inputs from mangroves and weaker brackish-water dilution relative to the seaward fringe, where strong estuarine mixing prevails. The porewater salinity at the landward sites was comparable to that of the coastal seawater measured during high tide (Fig. 2a), indicating that seawater intrusion reaches inland during flood tides. During the subsequent ebb tides, the influence of freshwater from the Chao Phraya River becomes stronger on the seaward (riverward) side, resulting in lower salinity at those sites. Tree biomass and fine-root density increase landward at this site (Hongwiset et al., 2022), potentially promoting sedimentary OC accumulation and, in turn, increasing DOM production through decomposition of sedimentary organic matter. Consistently, higher DIC concentrations at landward sites (Fig. 2h) indicate enhanced subsurface microbial decomposition and root respiration (Ray et al., 2020). Sulfate reduction may act as a dominant microbial degradation pathway in these sediments, generating alkalinity (bicarbonate) and thereby potentially increasing porewater DIC (Alongi, 2023; Reithmaier et al., 2023). Although sediment OC stocks generally increase with mangrove maturation (Carnell et al., 2022; Sharma et al., 2022; Ray et al., 2023) and biomass accumulation with forest age has been linked to higher DOC concentrations (Ray et al., 2023), no significant age-related trend in DOC was detected in this study. This discrepancy likely reflects the relatively short observation window (<10 years) compared with previous studies (<30 years) (Ray et al., 2023) and stronger tidal dilution and export of mangrove-derived DOM at the seaward sites, which reduced between-site contrasts. Overall, these results indicate that spatial variability in DOC concentrations at Bang Pu is governed more by tidal dilution and below-ground biomass than by forest age.

In the Bang Pu mangrove, porewater DOM molecular composition varied along the spatial gradient and with forest age (Fig. 5). NMDS results showed that AI_{mod} and DBE increased at landward sites in older stands (Fig. 5), suggesting that shifts in molecular composition were associated with an increasing contribution of structurally recalcitrant compounds (Koch and Dittmar, 2006; Li et al., 2025). Regardless of forest age, the relative abundance of aromatic compounds was lower at seaward sites, excluding the mudflat (Figs. 3i and 5), indicating efficient export of mangrove-derived compounds from the seaward zone via tidal pumping (Stieglitz et al., 2013; Mori et al., 2019; Xiao et al., 2023). Although aromatic compounds exhibit high photoreactivity after export to coastal waters (Dittmar et al., 2006; Tremblay et al., 2007; Kida et al., 2019b), their higher relative abundance at older sites within the

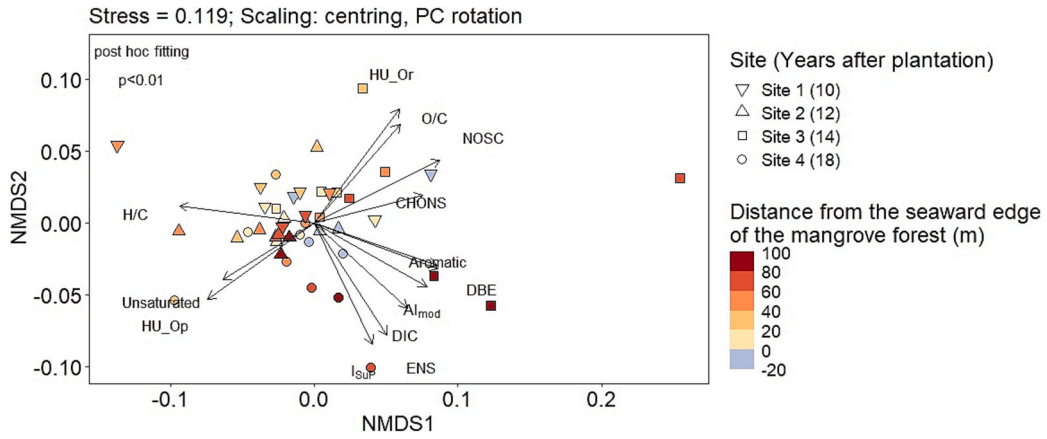


Fig. 5. Non-metric multidimensional scaling based on Jensen–Shannon divergence, calculated from the FT-ICR MS intensities. Color represents landward distances from the seaward edge of the mangrove forest, while the shapes represent sites with different years after plantation. Black arrows represent average molecular properties fitted *post-hoc* onto the two-dimensional ordination space ($p < 0.01$).

mangrove interior, where light availability is limited (Fig. 3i), likely reflects their resistance to microbial degradation (D'Andrilli et al., 2015) and higher below-ground biomass (Hongwiset et al., 2022). In contrast, the mudflat displayed distinct biogeochemical characteristics relative to the mangrove sites (Fig. 2), with elevated proportions of aromatic compounds (Fig. 3i), potentially reflecting non-mangrove sources such as wooden structures (for plantation activities) present on the mudflat and effluents from the Chao Phraya River (Boonyatumanond et al., 2006). The decrease in the relative abundance of CHON compounds at landward sites (Fig. 3b) further suggests a stronger contribution of marine-derived N-containing compounds in the seaward fringe (Knoke et al., 2024). Collectively, these results indicate that tidal dilution may homogenize porewater DOM composition in the seaward fringe, whereas mangrove-derived aromatic compounds increasingly dominate in older landward stands.

At landward sites in older plantations, the relative abundance of CHOS compounds increased in addition to aromatic compounds (Figs. 3c and 5). CHOS compounds are known to be abundant in mangrove porewaters (Mori et al., 2019; Knoke et al., 2024; Chen et al., 2025), and their enrichment supports the possibility of abiotic sulfurization of DOM (Gomez-Saez et al., 2016; Abdulla et al., 2020; Kurek et al., 2024). In the Bang Pu mangrove, sulfate-reducing conditions indicated by porewater pH and Eh (Fig. 2c and d) (Reef et al., 2010), together with the high sulfur content typical of mangrove sediments (Qian et al., 2024), create favorable conditions for abiotic sulfurization. Abiotic sulfurization of DOM has been widely reported in mangrove and coastal sediments (Schmidt et al., 2009; Seidel et al., 2014; Abdulla et al., 2020; Gomez-Saez et al., 2021; Zeller et al., 2024). On average, DOS accounted for 19% of the relative peak intensities and 25% of the molecular formula numbers, values comparable to those reported for other mangrove ecosystems. During abiotic sulfurization, reduced sulfur is randomly incorporated into DOM molecules, increasing functional group diversity, suppressing microbial degradation, and ultimately promoting DOM accumulation (Pohlabeln et al., 2017). Consistently, the widespread occurrence of DOS across all molecular classes (Fig. S2) further implies the involvement of abiotic sulfurization at this site, although further analysis would be required for confirmation. The concomitant increases in DOM molecular diversity and I_{SuP} at older landward sites suggest that mangrove-derived DOS contributes to DOM molecular diversification (Fig. 4). The mechanism driving this age-related increase in DOS likely involves the dynamics of reactive iron. Seawater-derived sulfate is reduced within mangrove sediments, producing polysulfides and sulfides that can cause abiotic sulfurization (Pohlabeln et al., 2017). However, reactive iron in the sediments and porewater preferentially reacts with these reduced sulfur species to form iron sulfides and pyrite (Canfield et al., 1992; Mori et al., 2019). Because sulfides react more readily with iron than with organic matter, abiotic sulfurization of organic matter may consequently be suppressed in environments rich in reactive iron (Abdulla et al., 2020; Zeller et al., 2024). At the Bang Pu site, we have observed that as the plantation age increases, reactive iron in the cc decreases while pyrite increases (unpublished data). This progressive depletion of reactive iron may provide a mechanistic explanation for the increase in DOS over time, as sulfides become increasingly available to react with DOM. In contrast, the absence of an age-related increase in CHOS compounds at seaward sites (Fig. 3c) suggests that strong tidal mixing facilitates the export of DOS to adjacent waters, limiting its accumulation in seaward porewaters. The pronounced increase in I_{SuP} at Sites 3 and 4 further indicates that abiotic sulfurization exerts a stronger influence on the DOM pool in the landward zone than at other sites (Fig. 4a). Overall, these results suggest that increasing plantation age in the landward mangrove enhances abiotic processes affecting DOM relative to seaward or younger forest sites.

It is important to acknowledge a few methodological limitations in this study. First, the results are derived from a single sampling event. The observed DOC concentrations may reflect a dynamic equilibrium between production and degradation. Consequently, a portion of the DOM constituents at sites with high DOC concentrations may be freshly produced by primary producers (mangrove roots and benthic algae) and thus labile and actively consumed by heterotrophic microbes. Second, the analytical workflow introduced some methodological biases. The solid-phase extraction required for desalination prior to FT-ICR MS analysis resulted in the loss of approximately half the porewater DOM in terms of DOC (Table S1), biasing towards more hydrophobic compounds that can be extracted by the resin. Furthermore, the use of negative-mode ESI precluded the detection of non-ionizable compounds in SPE-DOM (Patriarca et al., 2020). Future studies may benefit from a more quantitative approach, such as direct analysis by ^{1}H nuclear magnetic resonance spectroscopy (Fox et al., 2018; Kida et al., 2019a, 2023). Despite these constraints, this study successfully characterized the spatiotemporal variations in concentration and composition of porewater DOM. By elucidating DOM dynamics in a planted mangrove forest, this work provides valuable insights for future environmental research and management strategies.

5. Conclusion

In this study, we combined a chronosequence approach with ultrahigh-resolution analysis using FT-ICR MS in a planted mangrove forest in Thailand (10–18 years after plantation) to elucidate the spatiotemporal variability in porewater DOM concentration and

molecular composition. Porewater DOC concentrations were primarily controlled by the seaward-to-landward spatial environmental gradient, with no significant effect of forest age on a decadal scale, partly rejecting our initial hypothesis. This suggests that the DOC pool size is regulated more by physical and biological factors, such as tidal dilution effects and below-ground biomass, than by the stage of forest development. On the seaward side, active water exchange driven by tidal pumping likely facilitates the export of DOM to adjacent waters, thereby shaping the concentration gradient. The SPE-DOM molecular composition was influenced not only by the distance from the seaward edge but also by forest age. Specifically, at landward sites in older forests, the relative abundances of aromatic and CHOS compounds increased. Furthermore, an elevation in molecular diversity was observed concomitantly with the increase in mangrove-derived DOS. This suggests that in the interior of mature mangrove forests, abiotic sulfurization may proceed under sulfate-reducing environments, contributing to the accumulation of diverse and recalcitrant mangrove-derived DOM.

Importantly, despite the relatively narrow age gradient of our chronosequence (10–18 years after plantation), our results showed that mangrove development substantially alters the quality of porewater DOM (molecular composition and diversity) rather than its quantity (concentration), highlighting a decoupling between the two. In particular, the accumulation of recalcitrant compounds and the increase in molecular diversity with forest aging may provide a perspective for understanding long-term carbon sequestration mechanisms within mangrove sediments and the quality of DOM exported to adjacent coastal waters. This study emphasizes that integrating qualitative assessments at the molecular level and spatiotemporal perspectives, in addition to quantitative assessments of DOM, is essential for elucidating blue carbon dynamics in mangrove ecosystems.

Declaration of Generative AI and AI-assisted technologies in the writing process

During the preparation of this work the first author used Gemini (Google) in order to improve the readability. After using this tool, the author(s) reviewed and edited the content as needed and take full responsibility for the content of the published article.

Author contribution

RS and MK conducted all experiments and data analysis, with the help of KS for nutrient analysis and HN for FT-ICR MS analysis, respectively. RS wrote the initial draft under the supervision of MK. All authors participated in finalizing the manuscript.

CRediT authorship contribution statement

Ryu Sumioka: Writing – review & editing, Writing – original draft, Visualization, Software, Investigation, Formal analysis, Data curation. **Chadtip Rodtassana:** Writing – review & editing. **Sasitorn Poungparn:** Writing – review & editing, Project administration. **Hiroshi Nishimura:** Writing – review & editing, Resources. **Ken'ichi Shinozuka:** Writing – review & editing, Resources. **Toshiyuki Ohtsuka:** Writing – review & editing, Project administration, Funding acquisition. **Nobuhide Fujitake:** Writing – review & editing, Resources. **Morimaru Kida:** Writing – review & editing, Visualization, Supervision, Software, Project administration, Investigation, Funding acquisition, Formal analysis, Data curation, Conceptualization.

Declaration of competing interest

The authors declare that they have no known competing financial interests or personal relationships that could have appeared to influence the work reported in this paper.

Acknowledgments

The access to FT-ICR MS was provided by Analysis and Development System for Advanced Materials (ADAM) of RISH, Kyoto University, as a collaborative program. This study was supported by JSPS KAKENHI [grant numbers JP21KK0186 (TO) and JP24H01513 (MK)] and JST FOREST (Fusion Oriented REsearch for disruptive Science and Technology) Program [grant number JPMJFR231C (MK)].

Appendix A. Supplementary data

Supplementary data to this article can be found online at https://doi.org/10.1016/j.orggeochem.2026.105208.

Data availability

The dataset is freely available at figshare: https://doi.org/10.6084/m9.figshare.30286408.

References

Abdulla, H.A., Burdige, D.J., Komada, T., 2020. Abiotic formation of dissolved organic sulfur in anoxic sediments of Santa Barbara Basin. Organic Geochemistry 139, 103879. https://doi.org/10.1016/j.orggeochem.2019.05.009.

Alongi, D.M., 2023. Current status and emerging perspectives of coastal blue carbon ecosystems. Carbon Footprints 2, 12. https://doi.org/10.20517/cf.2023.04.

Alongi, D.M., 2020. Carbon cycling in the world's mangrove ecosystems revisited: significance of non-steady state diagenesis and subsurface linkages between the forest floor and the coastal ocean. Forests 11, 977. https://doi.org/10.3390/f11090977.

Arrieta, J.M., Mayol, E., Hansman, R.L., Herndl, G.J., Dittmar, T., Duarte, C.M., 2015. Dilution limits dissolved organic carbon utilization in the deep ocean. Science 348, 331–333. https://doi.org/10.1126/science.1258955.

Bauer, J.E., Cai, W.-J., Raymond, P.A., Bianchi, T.S., Hopkinson, C.S., Regnier, P.A.G., 2013. The changing carbon cycle of the coastal ocean. Nature 504, 61–70. https://doi.org/10.1038/nature12857.

Boonyatumanond, R., Wattayakorn, G., Togo, A., Takada, H., 2006. Distribution and origins of polycyclic aromatic hydrocarbons (PAHs) in riverine, estuarine, and marine sediments in Thailand. Marine Pollution Bulletin 52, 942–956. https://doi.org/10.1016/j.marpolbul.2005.12.015.

Bouillon, S., Borges, A.V., Castañeda-Moya, E., Diele, K., Dittmar, T., Duke, N.C., Kristensen, E., Lee, S.Y., Marchand, C., Middelburg, J.J., Rivera-Monroy, V.H., Smith III, T.J., Twilley, R.R., 2008. Mangrove production and carbon sinks: a revision of global budget estimates. Global Biogeochemical Cycles 22. https://doi.org/10.1029/2007GB003052.

Burke, P.M., Hill, S., Iricanin, N., Douglas, C., Essex, P., Tharin, D., 2002. Evaluation of preservation methods for nutrient species collected by automatic samplers. Environmental Monitoring and Assessment 80, 149–173. https://doi.org/10.1023/A:1020660124582.

Canfield, D.E., Raiswell, R., Bottrell, S.H., 1992. The reactivity of sedimentary iron minerals toward sulfide. American Journal of Science 292. https://doi.org/10.2475/ajs.292.9.659.

Cao, R., Chen, S., Yoshitake, S., Ohtsuka, T., 2019. Nitrogen deposition and responses of forest structure to nitrogen deposition in a cool-temperate deciduous forest. Forests 10, 631. https://doi.org/10.3390/f10080631.

Carnell, P.E., Palacios, M.M., Waryszak, P., Trevathan-Tackett, S.M., Masqué, P., Macreadie, P.I., 2022. Blue carbon drawdown by restored mangrove forests improves with age. Journal of Environmental Management 306, 114301. https://doi.org/10.1016/j.jenvman.2021.114301.

Chen, Z.L., Zhang, Z.-X., Cai, R., Yi, Y., Liang, W., Macreadie, P.I., Sanders, C.J., Lee, S.Y., Wang, F., He, D., 2025. Molecular fingerprints of sedimentary dissolved organic matter in mangroves: importance to blue carbon sequestration. Chemical Geology 671, 122495. https://doi.org/10.1016/j.chemgeo.2024.122495.

D'Andrilli, J., Cooper, W.T., Foreman, C.M., Marshall, A.G., 2015. An ultrahigh-resolution mass spectrometry index to estimate natural organic matter lability. Rapid Communications in Mass Spectrometry 29, 2385–2401. https://doi.org/10.1002/rcm.7400.

Dittmar, T., 2015. Reasons behind the long-term stability of dissolved organic matter. In: Hansell, D.A., Carlson, C.A. (Eds.), Biogeochemistry of Marine Dissolved Organic Matter. Elsevier, pp. 369–388. https://doi.org/10.1016/B978-0-12-405940-5.00007-8.

Dittmar, T., Hertkorn, N., Kattner, G., Lara, R.J., 2006. Mangroves, a major source of dissolved organic carbon to the oceans. Global Biogeochemical Cycles 20, 2005GB002570. https://doi.org/10.1029/2005GB002570.

Dittmar, T., Koch, B., Hertkorn, N., Kattner, G., 2008. A simple and efficient method for the solid-phase extraction of dissolved organic matter (SPE-DOM) from seawater. Limnology & Ocean Methods 6, 230–235. https://doi.org/10.4319/lom.2008.6.230.

Fox, C.A., Abdulla, H.A., Burdige, D.J., Lewicki, J.P., Komada, T., 2018. Composition of dissolved organic matter in pore waters of anoxic marine sediments analyzed by 1H

nuclear magnetic resonance spectroscopy. Frontiers in Marine Science 5. https://doi.org/10.3389/fmars.2018.00172.
Freeman, E.C., Peller, T., Altermatt, F., 2025. Ecosystem ecology needs an ecology of molecules. Trends in Ecology & Evolution 40, 219–223. https://doi.org/10.1016/j.tree.2024.12.006.
Gomez-Saez, G.V., Dittmar, T., Holtappels, M., Pohlabeln, A.M., Lichtschlag, A., Schnetger, B., Boetius, A., Niggemann, J., 2021. Sulfurization of dissolved organic matter in the anoxic water column of the Black Sea. Science Advances 7, eabf6199. https://doi.org/10.1126/sciadv.abf6199.
Gomez-Saez, G.V., Niggemann, J., Dittmar, T., Pohlabeln, A.M., Lang, S.Q., Noowong, A., Pichler, T., Wörmer, L., Bühring, S.I., 2016. Molecular evidence for abiotic sulfurization of dissolved organic matter in marine shallow hydrothermal systems. Geochimica et Cosmochimica Acta 190, 35–52. https://doi.org/10.1016/j.gca.2016.06.027.
He, D., Zhang, K., Cui, X., Tang, J., Sun, Y., 2018. Spatiotemporal variability of hydrocarbons in surface sediments from an intensively human-impacted Xiaoqing River-Laizhou Bay system in the eastern China: occurrence, compositional profile and source apportionment. Science of the Total Environment 645, 1172–1182. https://doi.org/10.1016/j.scitotenv.2018.07.193.
Herzsprung, P., Hertkorn, N., Von Tümpling, W., Harir, M., Friese, K., Schmitt-Kopplin, P., 2014. Understanding molecular formula assignment of Fourier transform ion cyclotron resonance mass spectrometry data of natural organic matter from a chemical point of view. Analytical and Bioanalytical Chemistry 406, 7977–7987. https://doi.org/10.1007/s00216-014-8249-y.
Hongwiset, S., Rodtassana, C., Poungparn, S., Umnouysin, S., Suchewaboripont, V., 2022. Synergetic roles of mangrove vegetation on sediment accretion in coastal mangrove plantations in central Thailand. Forests 13, 1739. https://doi.org/10.3390/f13101739.
Jaffé, R., McKnight, D., Maie, N., Cory, R., McDowell, W.H., Campbell, J.L., 2008. Spatial and temporal variations in DOM composition in ecosystems: the importance of long-term monitoring of optical properties. Journal of Geophysical Research: Biogeosciences 113. https://doi.org/10.1029/2008JG000683.
Jia, M., Wang, Z., Mao, D., Ren, C., Song, K., Zhao, C., Wang, C., Xiao, X., Wang, Y., 2023. Mapping global distribution of mangrove forests at 10-m resolution. Science Bulletin 68, 1306–1316. https://doi.org/10.1016/j.scib.2023.05.004.
Johnson, E.A., Miyanishi, K., 2008. Testing the assumptions of chronosequences in succession. Ecology Letters 11, 419–431. https://doi.org/10.1111/j.1461-0248.2008.01173.x.
Jost, L., 2007. Partitioning diversity into independent alpha and beta components. Ecology 88, 2427–2439. https://doi.org/10.1890/06-1736.1.
Jost, L., 2006. Entropy and diversity. Oikos 113, 363–375. https://doi.org/10.1111/j.2006.0030-1299.14714.x.
Kida, M., Fujitake, N., Kojima, T., Tanabe, Y., Hayashi, K., Kudoh, S., Dittmar, T., 2021. Dissolved organic matter processing in pristine antarctic streams. Environmental Science & Technology 55, 10175–10185. https://doi.org/10.1021/acs.est.1c03163.
Kida, M., Merder, J., Dittmar, T., Pawlowsky-Glahn, V., Egozcue, J.J., 2026. Reframing natural organic matter research through compositional data analysis. Frontiers in Environmental Science 14. https://doi.org/10.3389/fenvs.2026.1724142.
Kida, M., Merder, J., Fujitake, N., Tanabe, Y., Hayashi, K., Kudoh, S., Dittmar, T., 2023. Determinants of microbial-derived dissolved organic matter diversity in Antarctic Lakes. Environmental Science & Technology 57, 5464–5473. https://doi.org/10.1021/acs.est.3c00249.
Kida, M., Sato, H., Okumura, A., Igarashi, H., Fujitake, N., 2019a. Introduction of DEAE Sepharose for isolation of dissolved organic matter. Limnology 20, 153–162. https://doi.org/10.1007/s10201-018-0561-3.
Kida, M., Tanabe, M., Tomotsune, M., Yoshitake, S., Kinjo, K., Ohtsuka, T., Fujitake, N., 2019b. Changes in dissolved organic matter composition and dynamics in a subtropical mangrove river driven by rainfall. Estuarine, Coastal and Shelf Science 223, 6–17. https://doi.org/10.1016/j.ecss.2019.04.029.
Kida, M., Tomotsune, M., Iimura, Y., Kinjo, K., Ohtsuka, T., Fujitake, N., 2017. High salinity leads to accumulation of soil organic carbon in mangrove soil. Chemosphere 177, 51–55. https://doi.org/10.1016/j.chemosphere.2017.02.074.
Knoke, M., Dittmar, T., Zielinski, O., Kida, M., Asp, N.E., de Rezende, C.E., Schnetger, B., Seidel, M., 2024. Outwelling of reduced porewater drives the biogeochemistry of dissolved organic matter and trace metals in a major mangrove-fringed estuary in Amazonia. Limnology and Oceanography 69, 262–278. https://doi.org/10.1002/lno.12473.
Koch, B.P., Dittmar, T., 2016. From mass to structure: an aromaticity index for high-resolution mass data of natural organic matter. Rapid Communications in Mass Spectrometry 30, 250. https://doi.org/10.1002/rcm.7433.
Koch, B.P., Dittmar, T., 2006. From mass to structure: an aromaticity index for high-resolution mass data of natural organic matter. Rapid Communications in Mass Spectrometry 20, 926–932. https://doi.org/10.1002/rcm.2386.
Kurek, M.R., Wickland, K.P., Nichols, N.A., McKenna, A.M., Anderson, S.M., Dornblaser, M.M., Koupaei-Abyazani, N., Poulin, B.A., Bansal, S., Fellman, J.B., Druschel, G.K., Bernhardt, E.S., Spencer, R.G.M., 2024. Linking dissolved organic matter composition to landscape properties in wetlands across the United States of America. Global Biogeochemical Cycles 38, e2023GB007917. https://doi.org/10.1029/2023GB007917.
Li, P., Tang, S., Cai, R., Zhang, Z., He, C., Shi, Q., He, D., 2025. Molecular dynamics and factors governing recalcitrance of dissolved organic matter: insights from laboratory incubation and ultra-high resolution mass spectrometry. Science of the Total Environment 964, 178580. https://doi.org/10.1016/j.scitotenv.2025.178580.
Maher, D.T., Santos, I.R., Golsby-Smith, L., Gleeson, J., Eyre, B.D., 2013. Groundwater-derived dissolved inorganic and organic carbon exports from a mangrove tidal creek: the missing mangrove carbon sink? Limnology and Oceanography 58, 475–488. https://doi.org/10.4319/lo.2013.58.2.0475.
Mentges, A., Feenders, C., Seibt, M., Blasius, B., Dittmar, T., 2017. Functional molecular diversity of marine dissolved organic matter is reduced during degradation. Frontiers in Marine Science 4. https://doi.org/10.3389/fmars.2017.00194.
Merder, J., Freund, J.A., Feudel, U., Hansen, C.T., Hawkes, J.A., Jacob, B., Klaproth, K., Niggemann, J., Noriega-Ortega, B.E., Osterholz, H., Rossel, P.E., Seidel, M., Singer, G., Stubbins, A., Waska, H., Dittmar, T., 2020. ICBM-OCEAN: processing ultrahigh-resolution mass spectrometry data of complex molecular mixtures. Analytical Chemistry 92, 6832–6838. https://doi.org/10.1021/acs.analchem.9b05659.
Mori, C., Santos, I.R., Brumsack, H.-J., Schnetger, B., Dittmar, T., Seidel, M., 2019. Non-conservative behavior of dissolved organic matter and trace metals (Mn, Fe, Ba) driven by porewater exchange in a subtropical mangrove-estuary. Frontiers in Marine Science 6, 481. https://doi.org/10.3389/fmars.2019.00481.
Mouras, N., Lemonnier, H., Crossay, T., Gututauava, K., Mathian, M., Robin, S.L., Tardivel, O., Marchand, C., 2025. Variability of the optical signatures of dissolved organic matter in soils of different mangrove stands (Ouvéa, New Caledonia). Environmental Science and Pollution Research. https://doi.org/10.1007/s11356-025-36373-9.
Oksanen, J., Simpson, G.L., Blanchet, F.G., Kindt, R., Legendre, P., Minchin, P.R., O'Hara, R.B., Solymos, P., Stevens, M.H.H., Szoecs, E., Wagner, H., Barbour, M., Bedward, M., Bolker, B., Borcard, D., Carvalho, G., Chirico, M., De Caceres, M., Durand, S., Evangelista, H.B.A., FitzJohn, R., Friendly, M., Furneaux, B., Hannigan, G., Hill, M.O., Lahti, L., McGlinn, D., Ouellette, M.-H., Ribeiro Cunha, E., Smith, T., Stier, A., Ter Braak, C.J.F., Weedon, J., 2022. vegan: Community Ecology Package. Doi: 10.32614/CRAN.package.vegan.
Patriarca, C., Balderrama, A., Može, M., Sjöberg, P.J.R., Bergquist, J., Tranvik, L.J., Hawkes, J.A., 2020. Investigating the ionization of dissolved organic matter by electrospray. Analytical Chemistry 92, 14210–14218. https://doi.org/10.1021/acs.analchem.0c03438.
Pohlabeln, A.M., Gomez-Saez, G.V., Noriega-Ortega, B.E., Dittmar, T., 2017. Experimental evidence for abiotic sulfurization of marine dissolved organic matter. Frontiers in Marine Science 4. https://doi.org/10.3389/fmars.2017.00364.
Qian, L., Yan, B., Zhou, J., Fan, Y., Tao, M., Zhu, W., Wang, C., Tu, Q., Tian, Y., He, Q., Wu, K., Niu, M., Yan, Q., Nikoloski, Z., Liu, G., Yu, X., He, Z., 2024. Comprehensive profiles of sulfur cycling microbial communities along a mangrove sediment depth. Science of the Total Environment 944, 173961. https://doi.org/10.1016/j.scitotenv.2024.173961.
Ray, R., Suwa, R., Miyajima, T., Munar, J., Yoshikai, M., San Diego-McGlone, M.L., Nadaoka, K., 2023. Sedimentary blue carbon dynamics based on chronosequential observations in a tropical restored mangrove forest. Biogeosciences 20, 911–928. https://doi.org/10.5194/bg-20-911-2023.
Ray, R., Thouzeau, G., Walcker, R., Vantrepotte, V., Gleixner, G., Morvan, S., Devesa, J., Michaud, E., 2020. Mangrove-derived organic and inorganic carbon exchanges between the Sinnamary estuarine system (French Guiana, South America) and Atlantic Ocean. Journal of Geophysical Research: Biogeosciences 125, e2020JG005739. https://doi.org/10.1029/2020JG005739.
Reef, R., Feller, I.C., Lovelock, C.E., 2010. Nutrition of mangroves. Tree Physiology 30, 1148–1160. https://doi.org/10.1093/treephys/tpq048.
Reithmaier, G.M.S., Cabral, A., Akhand, A., Bogard, M.J., Borges, A.V., Bouillon, S., Burdige, D.J., Call, M., Chen, N., Chen, X., Cotovicz, L.C., Eagle, M.J., Kristensen, E., Kroeger, K.D., Lu, Z., Maher, D.T., Pérez-Lloréns, J.L., Ray, R., Taillardat, P., Tamborski, J.J., Upstill-Goddard, R.C., Wang, F., Wang, Z.A., Xiao, K., Yau, Y.Y.Y., Santos, I.R., 2023. Carbonate chemistry and carbon sequestration driven by inorganic carbon outwelling from mangroves and saltmarshes. Nature Communications 14, 8196. https://doi.org/10.1038/s41467-023-44037-w.
Riedel, T., Dittmar, T., 2014. A method detection limit for the analysis of natural organic matter via Fourier transform ion cyclotron resonance mass spectrometry. Analytical Chemistry 86, 8376–8382. https://doi.org/10.1021/ac501946m.
Santos, I.R., Burdige, D.J., Jennerjahn, T.C., Bouillon, S., Cabral, A., Serrano, O., Wernberg, T., Filbee-Dexter, K., Guimond, J.A., Tamborski, J.J., 2021. The renaissance of Odum's outwelling hypothesis in "Blue Carbon" science. Estuarine, Coastal and Shelf Science 255, 107361. https://doi.org/10.1016/j.ecss.2021.107361.
Schmidt, F., Elvert, M., Koch, B.P., Witt, M., Hinrichs, K.-U., 2009. Molecular characterization of dissolved organic matter in pore water of continental shelf sediments. Geochimica et Cosmochimica Acta 73, 3337–3358. https://doi.org/10.1016/j.gca.2009.03.008.
Seidel, M., Beck, M., Riedel, T., Waska, H., Suryaputra, I.G.N.A., Schnetger, B., Niggemann, J., Simon, M., Dittmar, T., 2014. Biogeochemistry of dissolved organic matter in an anoxic intertidal creek bank. Geochimica et Cosmochimica Acta 140, 418–434. https://doi.org/10.1016/j.gca.2014.05.038.
Sharma, S., Azman, M.S., Hamzah, M.L., Zakaria, R.M., Palaniveloo, K., MacKenzie, R.A., 2022. Total ecosystem blue carbon stocks and sequestration potential along a naturally regenerated mangrove forest chronosequence. SSRN Journal. https://doi.org/10.2139/ssrn.4179226.
Sharma, S., MacKenzie, R.A., Tieng, T., Soben, K., Tulyasuwan, N., Resanond, A., Blate, G., Litton, C.M., 2020. The impacts of degradation, deforestation and restoration on mangrove ecosystem carbon stocks across Cambodia. Science of the Total Environment 706, 135416. https://doi.org/10.1016/j.scitotenv.2019.135416.
Stieglitz, T.C., Clark, J.F., Hancock, G.J., 2013. The mangrove pump: the tidal flushing of animal burrows in a tropical mangrove forest determined from radionuclide budgets. Geochimica et Cosmochimica Acta 102, 12–22. https://doi.org/10.1016/j.gca.2012.10.033.

Tait, D.R., Maher, D.T., Macklin, P.A., Santos, I.R., 2016. Mangrove pore water exchange across a latitudinal gradient. Geophysical Research Letters 43, 3334–3341. https://doi.org/10.1002/2016GL068289.

Tanentzap, A.J., Fitch, A., Orland, C., Emilson, E.J.S., Yakimovich, K.M., Osterholz, H., Dittmar, T., 2019. Chemical and microbial diversity covary in fresh water to influence ecosystem functioning. Proceedings of the National Academy of Sciences 116, 24689–24695. https://doi.org/10.1073/pnas.1904896116.

Tanentzap, A.J., Fonvielle, J.A., 2024. Chemodiversity in freshwater health. Science 383, 1412–1414. https://doi.org/10.1126/science.adg8658.

Tremblay, L.B., Dittmar, T., Marshall, A.G., Cooper, W.J., Cooper, W.T., 2007. Molecular characterization of dissolved organic matter in a North Brazilian mangrove porewater and mangrove-fringed estuaries by ultrahigh resolution Fourier Transform-Ion Cyclotron Resonance mass spectrometry and excitation/emission spectroscopy. Marine Chemistry 105, 15–29. https://doi.org/10.1016/j.marchem.2006.12.015.

Walcker, R., Gandois, L., Proisy, C., Corenblit, D., Mougin, É., Laplanche, C., Ray, R., Fromard, F., 2018. Control of "blue carbon" storage by mangrove ageing: evidence from a 66-year chronosequence in French Guiana. Global Change Biology 24, 2325–2338. https://doi.org/10.1111/gcb.14100.

Walker, L.R., Wardle, D.A., Bardgett, R.D., Clarkson, B.D., 2010. The use of chronosequences in studies of ecological succession and soil development. Journal of Ecology 98, 725–736. https://doi.org/10.1111/j.1365-2745.2010.01664.x.

Wang, S., Liu, T., Zhu, E., He, C., Shi, Q., Feng, X., 2024. Potential retention of dissolved organic matter by soil minerals during wetland water-table fluctuations. Water Research 254, 121412. https://doi.org/10.1016/j.watres.2024.121412.

Wen, S., Hu, A., Jiang, S., Han, L., Jang, K.-S., Tanentzap, A.J., Zhong, J., Wang, J., 2024. Temperature sensitivity of organic carbon decomposition in lake sediments is mediated by chemodiversity. Global Change Biology 30, e17158. https://doi.org/10.1111/gcb.17158.

Xiao, K., Zhang, P., Santos, I.R., Wang, J.-J., Li, Z., Wang, X., Wang, Y.-H., Lu, M., Zhang, L., Li, H., 2023. Tidal pumping controls dissolved organic matter properties and outwelling from mangrove groundwater to coastal water. Water Resources Research 59, e2022WR033913. https://doi.org/10.1029/2022WR033913.

Zeller, M.A., Van Dam, B.R., Lopes, C., McKenna, A.M., Osburn, C.L., Fourqurean, J.W., Kominoski, J.S., Böttcher, M.E., 2024. The unique biogeochemical role of carbonate-associated organic matter in a subtropical seagrass meadow. Communications Earth & Environment 5, 1–13. https://doi.org/10.1038/s43247-024-01832-7.

Zhang, Y., Sun, Y., Liu, B., Wang, Y., Xie, W., Wang, P., Zhang, C., He, D., 2021. Spatiotemporal distribution and source variations of hydrocarbons in surface sediments from the Pearl River Estuary, Southern China. Journal of Soils and Sediments 21, 499–511. https://doi.org/10.1007/s11368-020-02783-0.